Received: 6 October 2022 | Revised: 14 February 2023 | Accepted: 18 February 2023

DOI: 10.1111/jnc.15792

Journal of Neurochemistry JNC The Official Journal of the International Society for Neurochemistry WILEY

ORIGINAL ARTICLE

Nimodipine accelerates the restoration of functional hyperemia during spreading oligemia

Ákos Menyhárt[1,2] | Armand Rafael Bálint[2,3] | Péter Kozák[2] | Ferenc Bari[3] | Eszter Farkas[1,2]

[1]Hungarian Centre of Excellence for Molecular Medicine—University of Szeged, Cerebral Blood Flow and Metabolism Research Group, Szeged, Hungary

[2]Department of Cell Biology and Molecular Medicine, Albert Szent-Györgyi Medical School and Faculty of Science and Informatics, University of Szeged, Szeged, Hungary

[3]Department of Medical Physics and Informatics, Albert Szent-Györgyi Medical School and Faculty of Science and Informatics, University of Szeged, Szeged, Hungary

Correspondence
Eszter Farkas, Department of Cell Biology and Molecular Medicine, Szent-Györgyi Albert Medical School, and Faculty of Science and Informatics, University of Szeged, Somogyi u. 4, H-6720 Szeged, Hungary.
Email: eszter.farkas@hcemm.eu

Funding information
EU's Horizon 2020 research and innovation program, Grant/Award Number: 739593; Ministry of Human Capacities of Hungary, Grant/Award Number: ÚNKP-20-4 -SZTE-153 and ÚNKP-22-2 -SZTE-225; Ministry of Innovation and Technology of Hungary and the National Research, Development and Innovation Fund, Grant/Award Number: TKP2021-EGA-28; National Research, Development and Innovation Office of Hungary, Grant/Award Number: K134334 and K134377; the University of Szeged Open Access Fund, Grant/Award Number: nr. 5978

Abstract

Spreading depolarization (SD) is assumed to be the pathophysiological correlate of migraine aura, leading to spreading depression of activity and a long-lasting vasoconstriction known as spreading oligemia. Furthermore, cerebrovascular reactivity is reversibly impaired after SD. Here, we explored the progressive restoration of impaired neurovascular coupling to somatosensory activation during spreading oligemia. Also, we evaluated whether nimodipine treatment accelerated the recovery of impaired neurovascular coupling after SD. Male, 4–9-month-old C57BL/6 mice ($n = 11$) were anesthetized with isoflurane (1%–1.5%), and SD was triggered with KCl through a burr hole made at the caudal parietal bone. EEG and cerebral blood flow (CBF) were recorded minimally invasively with a silver ball electrode and transcranial laser-Doppler flowmetry, rostral to SD elicitation. The L-type voltage-gated Ca^{2+} channel blocker nimodipine was administered i.p. (10 mg/kg). Whisker stimulation-related evoked potentials (EVPs) and functional hyperemia were assessed under isoflurane (0.1%)–medetomidine (0.1 mg/kg i.p.) anesthesia before, and repeatedly after SD, at 15-min intervals for 75 minutes. Nimodipine accelerated the recovery of CBF from spreading oligemia (time to full recovery, 52 ± 13 vs. 70 ± 8 min, nimodipine vs. control) and exhibited a tendency to shorten the duration of the SD-related EGG depression duration. The amplitudes of EVP and functional hyperemia were markedly reduced after SD, and progressively recovered over an hour post-SD. Nimodipine exerted no impact on EVP amplitude but consistently increased the absolute level of functional hyperemia from 20 min post-CSD (93 ± 11% vs. 66 ± 13%, nimodipine vs. control). A linear, positive correlation between EVP and functional hyperemia amplitude was skewed by nimodipine. In conclusion, nimodipine facilitated CBF restoration from spreading oligemia and the recovery of functional hyperemia post-SD, which were linked to a tendency of an accelerated return of spontaneous neural activity after SD. The use of nimodipine in migraine prophylaxis is suggested to be re-visited.

Abbreviations: 20-HETE, 20-hydroxy-eicosatetraenoic acid; aCSF, artificial cerebrospinal fluid; ANCOVA, analysis of covariance; BOLD MRI, blood-oxygen-level-dependent magnetic resonance imaging; CBF, cerebral blood flow; CGRP, calcitonin gene-related peptide; COX, cyclooxygenase; CVR, cerebrovascular reactivity; EEG, electroencephalogram; EVP, somatosensory evoked potential; LDF, Laser-Doppler flowmetry; PET, positron emission tomography; SAH, subarachnoid hemorrhage; SD, spreading depolarization; SPECT, single photon emission computed tomography; VGCC, voltage-gated calcium channel.

This article is part of the special issue "14th International Conference on Brain Energy Metabolism: Energy Substrates and Microbiome Govern Brain Bioenergetics and Cognitive Function with Aging".

KEYWORDS
cerebral blood flow, migraine with aura, neurovascular coupling, nimodipine, spreading depolarization, spreading oligemia

1 | INTRODUCTION

A longstanding assumption posits that the mechanism underlying migraine aura is spreading depolarization (SD) (Lauritzen, 1994; Leao & Morison, 1945). In support of the view that SD is related to migraine aura, the cerebral blood flow (CBF) response coupled with SD—especially its concluding spreading oligemic element—has been identified in migraine patients with single photon emission computed tomography (SPECT), positron emission tomography (PET), or blood-oxygen-level-dependent magnetic resonance imaging (BOLD MRI) (Hadjikhani et al., 2001; Lauritzen et al., 1983; Olesen et al., 1981; Woods et al., 1994). In addition to regular auras, some auras recorded in these imaging studies were probably triggered by cerebral microemboli emerging during the intracarotid injection of the tracer (Lauritzen et al., 1983; Olesen et al., 1981). In further support of the link between migraine and SD, transgenic experimental models of familial hemiplegic migraine (FHM) display increased SD susceptibility (Unekawa et al., 2018; van den Maagdenberg et al., 2004). Also, experimentally triggered SD in mice has recently been linked to trigeminal pain and anxiety (Harriott et al., 2021). Collectively, mounting clinical and experimental observations suggest that SD is highly likely the cause of migraine aura and may also trigger trigeminal sensory activation to initiate headache pain (Brennan & Pietrobon, 2018).

SD is a transient (0.5–1 min) mass depolarization of a critical tissue volume that propagates at a low rate of millimeters per minute in the gray matter (Somjen, 2001). In visual aura experience, a narrow scintillating rim moving over the visual field is followed by a scotoma. While the scintillating rim is thought to correspond to a high-frequency burst of population spikes (Herreras et al., 1994), the blind field represents SD, outlasted by a prolonged (5–15 min) depression of spontaneous activity (Lashley, 1941; Lauritzen, 1994; Leao, 1944; Milner, 1958). SD, together with the successive activity depression appears as a transient signal intensity attenuation or power reduction in the full band electrocorticogram, propagating from one contact point to the next (Leao, 1944).

SD is accompanied by a typical CBF response starting with a variable, short drop of CBF (early hypoperfusion) and dominated by a subsequent, large, transient hyperemia in naïve, optimally perfused tissue. In the mouse, the initial drop of CBF is more prominent than in phylogenetically higher mammals, and the upcoming hyperemia barely reaches pre-SD baseline CBF (Ayata et al., 2004). As noted above, the response is concluded by long-lasting oligemia subject to variations depending on the species, type of anesthesia, and other conditions (Ayata & Lauritzen, 2015). Spreading oligemia is also a surrogate phenomenon to enable the detection of SD with neuroimaging in migraine patients (Hadjikhani et al., 2001; Olesen et al., 1981). Furthermore, the oligemic phase of the CBF response appears to be coincident with the reversible impairment of cerebrovascular reactivity (CVR) to a hypercapnic challenge in anesthetized rodents (Fabricius et al., 1995; Florence et al., 1994; Lacombe et al., 1992; Wahl et al., 1987). Similarly, diminishing CVR with breath holding was measured during the inter-ictal periods in migraineurs (Akin & Bilensoy, 2006; Dzator et al., 2021). In addition to CVR, SD has also been shown to impair neurovascular coupling achieved by subtantia innominata stimulation (Lacombe et al., 1992), infraorbital nerve stimulation (Enager et al., 2004), transcallosal fiber stimulation (Piilgaard & Lauritzen, 2009), or optogenetic activation of the barrel cortex (Böhm et al., 2020).

There is persistent need to treat cerebrovascular disorders with pharmacological means. Nimodipine, an L-type voltage-gated calcium channel (VGCC) blocker is an approved agent with high affinity to L-type VGCCs on cerebrovascular smooth muscle cells (Freedman & Waters, 1987), and is clinically applied to prevent delayed ischemic deficit after subarachnoid hemorrhage (SAH) (Carlson et al., 2020). Importantly, recent clinical studies have associated the development of delayed ischemic deficit with SD occurrence (Dreier et al., 2022; Lückl et al., 2018). Prophylactic nimodipine may prevent poor outcome related to delayed cerebral ischemia in some SAH patients (Feigin et al., 1998), possibly by targeting the CBF response to SD (Dreier et al., 1998; Menyhárt et al., 2018; Windmuller et al., 2005). In the management of migraine, prophylactic treatment with nimodipine appeared effective at reducing migraine headache frequency and severity in some trials (Gelmers, 1983; Havanka-Kanniainen et al., 1985). Yet, nimodipine achieved small or no effect in other trials ("European multicenter trial of nimodipine in the prophylaxis of classic migraine (migraine with aura). Migraine-Nimodipine European Study Group (MINES)," 1989a; "European multicenter trial of nimodipine in the prophylaxis of common migraine (migraine without aura). Migraine-Nimodipine European Study Group (MINES)," 1989b), and the assessment of its efficacy was complicated by a high degree of placebo responders (Toldo et al., 2012). Treating migraine with nimodipine in the 1980s centered on the concept that migraine was primarily a cerebrovascular disorder (Leone et al., 1990). With the advanced understanding of the role of SD in migraine, nimodipine application in migraine management is worth re-examination (Carlson et al., 2020).

In the present study, we set out to explore the dysfunction and progressive restoration of neurovascular coupling with somatosensory stimulation after SD, with the aim to screen the temporal resolution of SD-related impairment. The efficacy of neurovascular coupling associated with somatosensory stimulation was assessed repeatedly over 75 min following SD. Importantly, we investigated the possibility to accelerate the recovery of impaired neurovascular coupling by pharmacological means. To this end, we applied nimodipine known to potentiate both functional hyperemia to

somatosensory stimulation (Szabó et al., 2019) and the CBF response coupled with SD (Menyhárt et al., 2018; Szabó et al., 2019). Also, we explored nimodipine action on the SD-associated EEG depression and the coupled CBF response. The results here may present new indications to re-visit the use of nimodipine in the clinical management of migraine with aura.

2 | METHODS

The ethical approach conformed to previously reported guidelines (Szabó et al., 2021; Toth et al., 2021), and the experiments are reported in compliance with the ARRIVE guidelines (Percie du Sert et al., 2020). The experimental procedures were approved by the National Food Chain Safety and Animal Health Directorate of Csongrád County, Hungary, and were performed according to the guidelines of the Scientific Committee of Animal Experimentation of the Hungarian Academy of Sciences (updated Law and Regulations on Animal Protection: 40/2013. (II. 14.) Gov. of Hungary), following the EU Directive 2010/63/EU on the protection (Ref. nr. XXXII/4050/2020 and I-74-23/2022. MÁB).

The animals were housed according to standard conditions reported earlier (Szabó et al., 2021; R. Toth et al., 2021). Adult male 4–4.5-month-old C57BL/6 mice (26 ± 33 g, n = 11, Charles River Laboratories, from the husbandry of the Biological Research Centre, Szeged, Hungary) were used in this study. No SD-related sexual dimorphism has been expected (Balkaya et al., 2019; Harriott et al., 2021). Standard rodent chow and tap water were supplied ad libitum. The animals were housed under constant temperature, humidity, and lighting conditions (23°C, 12:12 h light/dark cycle, lights on at 7 a.m.).

The estimation of sample size adhered to previously applied principles (Menyhárt et al., 2021; Szabó et al., 2021). Our pilot experiments indicated differences between the experimental groups (nimodipine vs. control) and reached the confidence level of 95% and a power of 80% at low sample size ($\alpha = 0.05$). To support 80% power, the animal number was at least 5 animals/group. Statistical analyses were conducted in SigmaPlot 12.5 (Systat Software, Inc., San Jose, CA, USA), sample size calculation and power analysis were run in GPower 3.1 (Heinrich Heine University of Düsseldorf, Germany).

Mice were arbitrarily taken from the animal housing facility to be prepared for experiments. The experiments were conducted during the light phase of the daily cycle. The mice were anesthetized with 1.5–2% isoflurane in N_2O:O_2 (2:1), mounted on a stereotactic frame and were allowed to breathe spontaneously through a head cone during surgical interventions. Body temperature was kept at 37.2°C by a feedback-controlled heating pad (Harvard Apparatus, Holliston, MA, U.S.A.). The skin on the skull was retracted and the right parietal bone was thinned under saline cooling with a high-precision electrical drill (ProLab Basic, Bien Air 810, Switzerland). Lidocaine (EGIS, Cat. Nr. OGYI-T-3047/03) was administered locally for pain relief. A small craniotomy was created at the caudal edge of the parietal bone for the induction of SD. The craniotomy was constantly kept moist by artificial cerebrospinal fluid (aCSF; mM concentrations: 126.6 NaCl, 3 KCl, 1.5 $CaCl_2$, 1.2 $MgCl_2$, 24.5 $NaHCO_3$, 6.7 urea, 3.7 glucose bubbled with 95% O_2 and 5% CO_2 to achieve a constant pH of 7.4).

For the minimally invasive recording of EEG and CBF, a silver ball electrode (Ag/AgCl reference electrode, WPI Instruments, Sarasota, USA) and a Laser-Doppler needle probe (Probe 403 connected to PeriFlux 5000; Perimed AB, Sweden) were positioned adjacent to each other on the thinned skull above the somatosensory cortex representing the vibrissae. An Ag/AgCl reference electrode was implanted under the skin of the animal's neck. The electrophysiological signal was recorded via a high input impedance head stage (NL100AK, NeuroLog System, Digitimer Ltd., United Kingdom), connected to an AC coupled pre-amplifier (NL104, NeuroLog System, Digitimer Ltd., United Kingdom) and a differential amplifier (NL106 NeuroLog System, Digitimer Ltd., United Kingdom) with associated filter modules (EEG filtered in wideband range: >1 Hz, NL125 NeuroLog System, Digitimer Ltd., United Kingdom) and conditioner systems (NL530, NeuroLog System, Digitimer Ltd., United Kingdom). Electrical signals were digitalized at a sampling frequency of 1 kHz by a dedicated data acquisition device (MP150, Biopac Systems, Inc., USA) controlled through the Acknowledge software (Acknowledge 4.2, Biopac Systems, Inc., USA). Laser-Doppler flowmetry (LDF) was used to record changes in local CBF. The LDF signal was digitalized and acquired, together with the EEG, essentially as described above.

EEG was used to confirm successful SD initiation, and the quantitative evaluation of the SD-related EEG depression and somatosensory evoked potentials (EVP). Somatosensory stimulation was achieved by the mechanical stimulation of the entire, intact (no trimming), left vibrissal pad at 2 Hz for 30 s by a custom-made device. The stimulation was repeated twice 2 min apart in a block of stimulation.

Before data acquisition the concentration of inhaled isoflurane was reduced to 0.3%–0.1%, and medetomidine was applied (0.5 mg/kg, i.p., twice at a 10 min interval) to complement anesthesia. This approach allowed the reliable evolution of functional hyperemia. After recording baseline EEG and CBF for 10 min, the first block of vibrissal pad stimulation was performed. Ten minutes later, SD was triggered by placing a tiny piece of filter paper (1 mm × 1 mm) soaked in 1 M KCl in the craniotomy. The filter paper was removed when EEG depression was seen, and the craniotomy was rinsed with aCSF to prevent the occurrence of further SD events. Over the next 75 min, vibrissal pad stimulation blocks were repeated first 2 times at an interval of 10 min, then an additional 2 times at an interval of 15 min. Shortly after the last block of stimulation, the experiments were terminated by overdosing isoflurane (5%), and data acquisition was suspended 10 min after cardiac arrest. The experimental protocol is illustrated in representative recordings (Figure 1).

Nimodipine (Sigma, Cat. Nr. N149-100 mg), an L-type voltage-gated calcium channel blocker was administered to some mice (n = 6; 10 mg/kg, 500 μL, i.p. bolus) (Ahmadi et al., 2012; Ingwersen et al., 2018) (Ahmadi et al., 2012; Ingwersen et al., 2018), 10–12 min before SD initiation and about 20 min before the first block

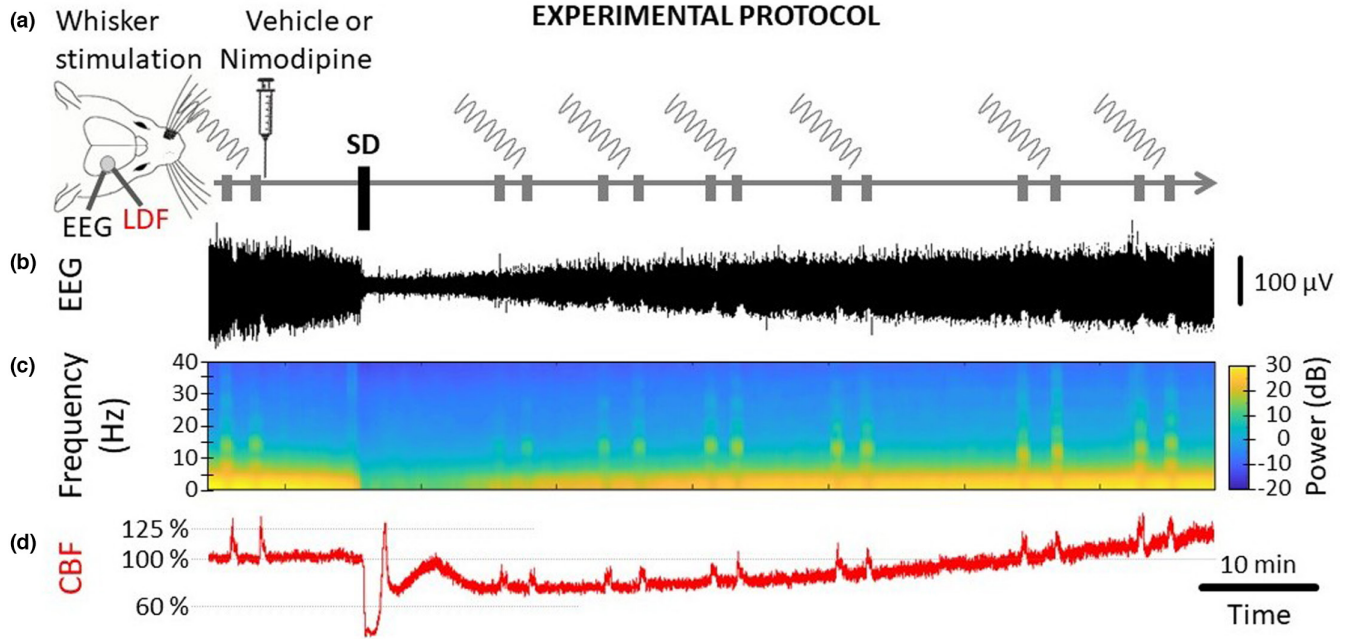

FIGURE 1 Experimental protocol (a) illustrated by a representative electroencephalogram (EEG) (b) and the corresponding power spectrum (c) to show the spontaneous depression of electrical activity associated with spreading depolarization (SD), as well as the signature of mechanical whisker stimulation performed twice in a stimulation block. The EEG signal was acquired via a silver ball electrode placed on the thinned skull surface. The corresponding red trace (d) indicates local cerebral blood flow (CBF) changes acquired with transcranial laser Doppler flowmetry (LDF) using a needle probe adjacent to the EEG electrode over the somatosensory cortex of an anesthetized mouse.

of somatosensory stimulation subsequent to SD ($n = 6$) (Figure 1). Every other mouse received vehicle (0.1% DMSO in saline, VWR Chemicals, Cat. Nr. 23500.260) in an equal volume and used as control ($n = 5$).

Variables (i.e., the EEG and LDF signals) were simultaneously acquired, displayed live, and stored using a personal computer equipped with the software AcqKnowledge 4.2 for MP 150 (Biopac Systems, Inc., Goleta, USA). Data analysis was assisted by the inbuilt instructions of the software AcqKnowledge 4.2. EVPs during whisker stimulation were analyzed in the original LFP recordings acquired at 1 kHz. Raw LDF recordings were downsampled to 1 Hz and then expressed relative to baseline by using the average CBF value of the first 5 minutes (100%) and the recorded biological zero obtained after terminating each experiment (0%) as reference points.

The experimenter was aware of the animal's group during experimentation. Data analysis was performed by another investigator, blind to the experimental condition (experimental group assignment was performed by a different person than the data analyst). No animal was excluded from the analysis.

The SD-related EEG depression and EEG recovery, as well as the potential drug effect were characterized by the EEG power taken over 1-min-long epochs prior to whisker stimulation blocks, at segments free of any noise. Also, the delay from SD induction to the recovery of EEG activity to 50 and 75% amplitude was taken as readouts of the duration of the SD-related EEG depression. As reported earlier (Szabó et al., 2019), it was required for EVPs that the segment under analysis (10 s) was completely free of harmonic network oscillations (~50 Hz, produced by the feedback controlled on–off switch of the heating blanket) or any accidental noise produced by manipulations by the experimenter. The peak amplitude of EVPs was assessed to reveal SD-related change or drug effect, if any.

CBF changes were expressed relative to baseline by using the average CBF of the first 5 minutes of baseline taken before the first whisker stimulation block (100%) and the recorded biological zero after terminating each experiment (0%). Resting CBF between stimulations was measured as the mean of the same epochs used for the calculation of EEG power. The efficacy of functional hyperemia to somatosensory stimulation was characterized by measuring the maximum amplitude of the CBF response (mean of the plateau of the hyperemic response).

Data are given as mean ± stdev. Statistical analysis was conducted according to established standards (Menyhárt et al., 2021; Szabó et al., 2019; Toth et al., 2021) with the software IBM SPSS 29 (Armonk, NY: IBM Corporation, U.S.A.) and SigmaPlot 12.5 (Systat Software, Inc., San Jose, CA, USA). No test for outliers was conducted; all data were used for statistical analysis. The distribution of the data was tested with a Shapiro–Wilk normality test. Since all datasets passed the normality test, we proceeded with a repeated measures paradigm followed by a Sidak post hoc test. Simple group comparisons were evaluated with a Student or a Welch independent samples *t*-test. Correlation analysis was conducted with a Pearson two-tailed model. Further analysis and comparison of regression lines was achieved with an analysis of covariance (ANCOVA) model. Levels of significance were set at $p < 0.05^{*}$ or $p < 0.01^{**}$. Distinct statistical methods are provided in each Figure legend.

3 | RESULTS

3.1 | The SD-related EEG depression and spreading oligemia

We recorded here EEG to disclose the signature of SD. In each experiment, SD was confirmed in the EEG recording (Leao, 1944), and the characteristic CBF response in the CBF traces (Ayata et al., 2004; Ayata & Lauritzen, 2015). The SD-related EEG depression and EEG recovery, as well as the potential drug effect were characterized by the EEG power taken over defined epochs prior to whisker stimulation blocks, and the time taken for the EEG activity to recover from the depression to 50% and 75% amplitude. (Figure 2). The EEG was depressed significantly up to 10 min after SD induction (EEG power: 32.4 ± 14.2 and 40.6 ± 24.2% of baseline; minimum activity and 10 min after SD onset, respectively). Its gradual recovery was confirmed by the return of the EEG power approaching pre-SD baseline, increasingly more obvious starting from 20 min after SD induction (53.0% ± 30.2% of baseline) (Figure 2a). Nimodipine did not facilitate the recovery of EEG activity from SD significantly at this sample size (Figure 2b). The non-significant but consistent nimodipine effect was corresponding to shorter time taken after SD induction to reach 50% and 75% of the pre-SD EEG amplitude as compared to control (50%, 11 ± 3 vs. 29 ± 22 min; 75%, 19 ± 10 vs. 43 ± 29 min, nimodipine vs. control) (Figure 2b).

Baseline CBF was level (not rising) before the first whisker stimulation block, and between the first whisker stimulation block and SD in both the control and nimodipine-treated groups. The CBF response to SD evolved in line with the known kinetics in the intact mouse cerebral cortex (Ayata et al., 2004)(Figure 1). An early hypoperfusion transient was followed by a hyperemic component (Figures 1 and 2c), the hyperemic peak occasionally falling short of pre-SD baseline CBF (Figure 2d). Nimodipine moderated the early hypoperfusion element, as reflected by the smaller drop of CBF (to 46.3 ± 14.7% vs. 20.8 ± 12.7%, nimodipine vs. control) (Figure 2e), but exerted no improvement on the hyperemic phase of the CBF

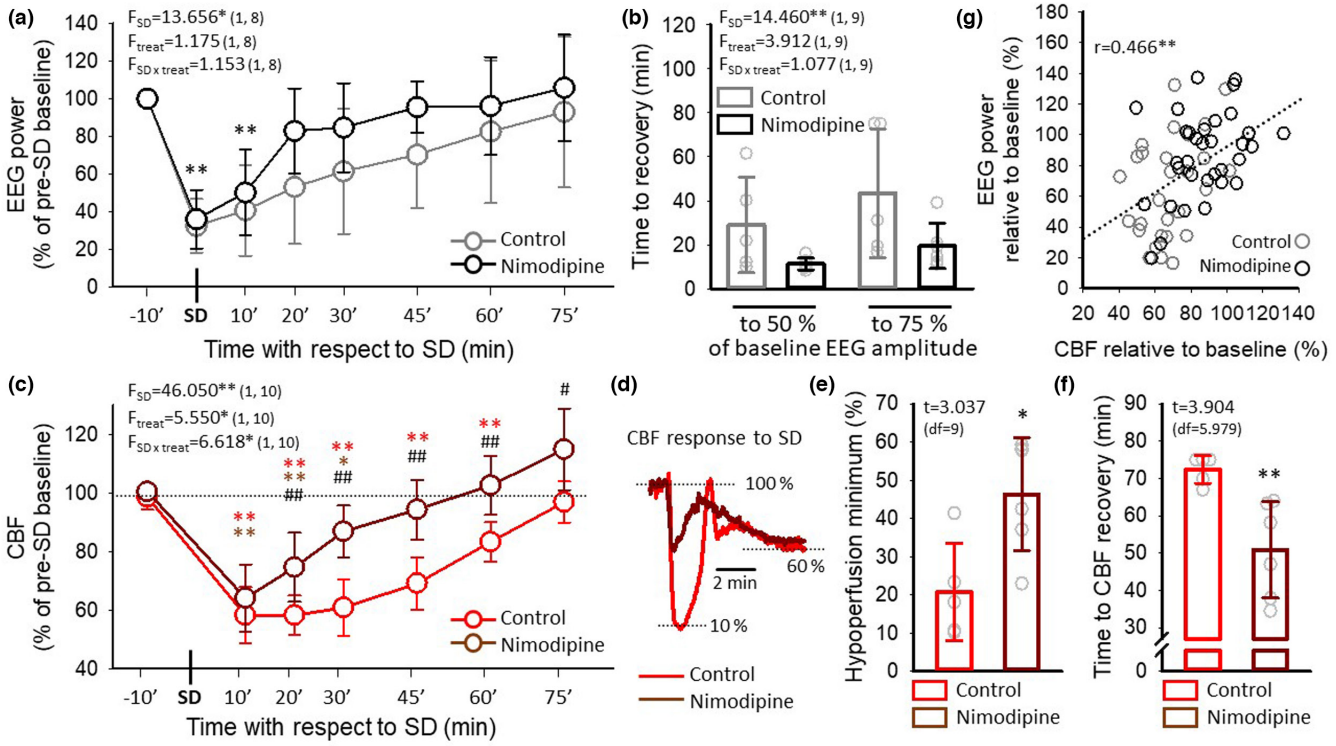

FIGURE 2 Spreading depolarization (SD) recognized by EEG power reduction, and the associated spreading oligemia after SD elicitation. (a) EEG power relative to baseline, sampled at the minimum of the SD-related EEG depression, before (−10 min) and after SD initiation (10–75 min). (b) Time taken for the EEG activity to recover from the depression to 50% and 75% amplitude. (c) Cerebral blood flow (CBF) changes relative to baseline, before (−10 min), and after SD elicitation (10–75 min) (scatter plot). (d) Traces representative of the CBF response to SD in a control and a nimodipine-treated mouse. (e) CBF minimum reached during the early hypoperfusion element of the CBF response to SD. (f) Time taken for CBF to recover to baseline (prior to SD elicitation). (g) Correlation between CBF and EEG power analyzed with two-tailed Pearson correlation, $p < 0.01^{**}$. Data in (a–c) and (e, f) are expressed as mean ± stdev; a Shapiro–Wilk test confirmed normal distribution for all datasets. In (a–c), a two-way ANOVA paradigm considering the impact of SD and treatment was applied for statistical analysis ($p < 0.05^{*}$ and $p < 0.01^{**}$) followed by a Sidak post hoc test ($p < 0.05^{*}$ & 0.01^{**} vs. pre-SD, and $p < 0.05^{\#}$ & $p < 0.01^{\#\#}$ nimodipine vs. respective control). In (e), an independent samples Student's *t*-test was used ($p < 0.05^{*}$). In (f) Welch independent samples *t*-test was used (and $p < 0.01^{**}$). Degrees of freedom are given next to the statistic output in brackets in all panels.

response. SD was followed by a prominent spreading oligemia (CBF minimum of 56.3 ± 10.3% relative to baseline) (Figures 1 and 2c)—the concluding element of the CBF response (Ayata & Lauritzen, 2015). Nimodipine administration did not affect the oligemic CBF minimum (52.4 ± 23.4% and 56.3 ± 10.3%, nimodipine and control).

CBF taken between somatosensory stimulations over the post-SD oligemia approached baseline gradually (Figure 2c). CBF did not return completely to pre-SD baseline over the 75 min period after SD elicitation in three mice in the control group. The delay to full CBF recovery required more than 65 min in two additional mice. In contrast, CBF in the nimodipine group was not significantly lower than baseline 45 min after SD initiation (Figure 2c) and fully recovered with a delay of 51 ± 13 min (Figure 2f). In fact, CBF in the nimodipine-treated animals was markedly improved compared to controls from 20 min after triggering SD (74.6 ± 11.8 vs. 58.3 ± 6.7, nimodipine vs. control) (Figure 2c). Finally, the level of CBF and the corresponding EEG power displayed a good positive linear correlation (Figure 2g).

3.2 | Somatosensory evoked field potentials and functional hyperemia

The amplitude of EVPs is known to be proportional to the number of neurons firing or the strength of subthreshold postsynaptic currents in the dendrites of a neuronal population (Langdon & Sur, 1990). In our experiments, EVP amplitude 10 min after SD elicitation was reduced to half of the pre-SD value (128.3 ± 35.2 vs. 241.7 ± 37.8 μV, 10 min vs. −10 min with respect to SD). EVP amplitude returned to baseline 60 min after SD initiation (213.7 ± 48.7 and 241.7 ± 37.8 μV, 60 min and −10 min with respect to SD elicitation). Nimodipine treatment exerted no effect on EVP amplitudes (Figure 3a,b).

Functional hyperemia to somatosensory stimulation was characterized by its absolute amplitude (peak relative to pre-SD baseline) and relative amplitude (difference between pre-stimulation baseline-to-peak). Both the absolute and relative amplitude of functional hyperemia proved to be considerably impaired shortly after SD elicitation (absolute, 75.7 ± 17.1% vs. 125.8 ± 14.9%; relative, 14.8 ± 10.1%

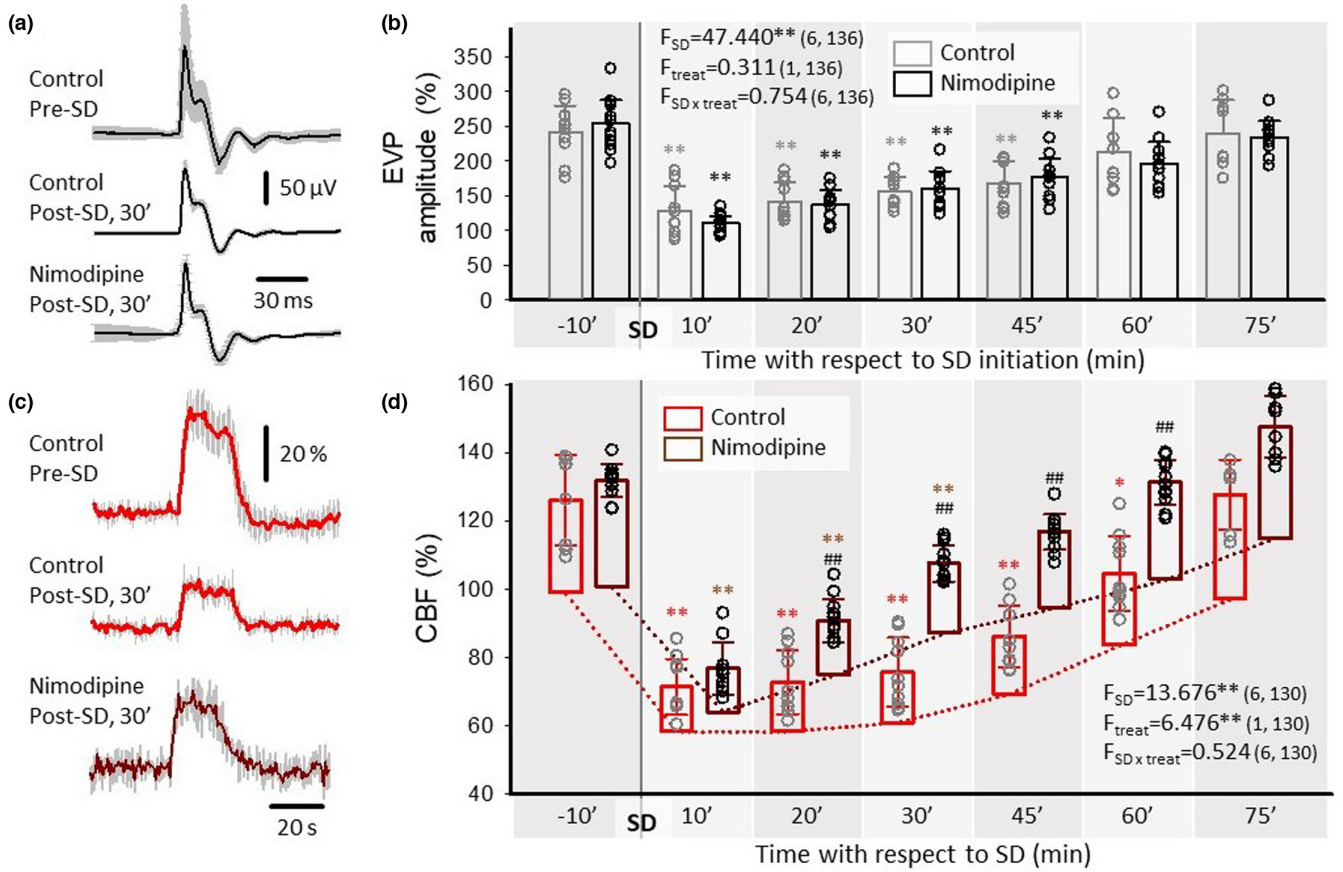

FIGURE 3 The impact of spreading depolarization (SD) and nimodipine treatment on somatosensory evoked potentials (EVPs) and associated functional hyperemia. (a) Electrocorticographic EVP signatures are shown as mean ± stdev of all analyzed events. (b) EVP amplitude before (−10 min) and after SD elicitation (10–75 min). (c) Laser-Doppler flowmetry signatures of functional hyperemia shown as mean ± stdev of all analyzed events. (d) Relative functional hyperemia amplitudes (height of bars) fitted on the corresponding pre-stimulation CBF level to appreciate absolute hyperemia amplitudes (top of the bars). Data in (b) and (d) are given as mean ± stdev; a Shapiro–Wilk test confirmed normal distribution for all data sets. A two-way ANOVA paradigm considering the impact of SD and treatment was applied for statistical analysis ($p < 0.05^{*}$ and $p < 0.01^{**}$) followed by a Sidak post hoc test ($p < 0.05^{*}$ and 0.01^{**} vs. pre-SD, and $p < 0.01^{\#\#}$ nimodipine vs. respective control). In (d), statistics for the absolute amplitude of functional hyperemia are shown. Degrees of freedom are given next to the statistic output in brackets in both panels.

vs. 27.1 ± 13.1%; 10 vs. −10 min with respect to SD) (Figure 3c,d). The absolute amplitude of functional hyperemia recovered to the optimal amplitude taken during baseline 75 min after SD initiation in the control group, and as early as 45 min in the nimodipine-treated group (Figure 3d). Furthermore, nimodipine considerably increased the absolute amplitude of hyperemia compared to control between 20 and 60 min after SD initiation (e.g., at 30 min: 107.2 ± 10.8% vs. 75.7 ± 17.1%, nimodipine vs. control) (Figure 3d). Yet, no direct impact of nimodipine was statistically confirmed on the relative amplitude of functional hyperemia (repeated measures: $F_{treat} = 0.225$).

Finally, we set out to explore whether resting CBF predicted the strength of neuronal activation in response to stimulus, and whether the efficacy of neurovascular coupling (i.e., greater neuronal activity coupled by greater CBF response (Fox & Raichle, 1985)) was altered by nimodipine treatment. Accordingly, the amplitude of EVP was correlated with pre-stimulus CBF and the relative amplitude of the corresponding functional hyperemia. A significant, positive, linear correlation was found between resting CBF prior to stimulation and EVP amplitude in both the control and nimodipine groups (Figure 4a). Furthermore, a potential nimodipine effect drawn from the comparison of the regression lines was tackled with an ANCOVA model. No difference between the slopes was indicated ($F = 0.189$, $p = 0.655$), but a group effect was seen in the intercept ($F = 30.533$, $p < 0.01^{**}$).

The relative amplitude of functional hyperemia increased with greater EVP amplitude in a linear fashion (Figure 4b). Comparison of the regression lines for the control and nimodipine groups with ANCOVA disclosed that the two lines were not parallel ($F = 3.862$, $p = 0.051$).

4 | DISCUSSION

4.1 | The efficacy of neurovascular coupling in the wake of spreading depolarization

Neurovascular coupling, the signaling mechanism that links functional hyperemia to increased neural activity is a measure of cerebrovascular health (Stackhouse & Mishra, 2021). Furthermore, local CBF increase serves as a surrogate measure of neural activity in noninvasive clinical neuroimaging (i.e., BOLD MRI) (Howarth et al., 2021). Here, we present that functional hyperemia in response to somatosensory stimulation becomes markedly attenuated following SD, with gradual recovery to pre-SD magnitude over the first hour post-SD (Figure 3). Also, the suppression of neuronal activity was clearly reflected by the decreased amplitude of EVPs after SD (Figure 3), coincident with the degree of spreading oligemia (Figure 4). This stands in line with a previous experimental observation that the CBF response to neuronal activation achieved with transcallosal electric stimulation declined (Piilgaard & Lauritzen, 2009), and the amplitude of EVP triggered by infraorbital nerve or transcallosal stimulation decreased after SD (Enager et al., 2004; Piilgaard & Lauritzen, 2009). The weakened hyperemic response observed here may be considered analogous to reduced baseline-to-peak changes of the functional near infrared spectroscopy (fNIRS) signal in sporadic hemiplegic migraine patients during a finger opposition task (Lo et al., 2020). A recent meta-analysis cautiously suggests that neurovascular coupling in migraine patients appears to be impaired, but calls for future confirmatory studies (Dzator et al., 2021). Our experimental findings on the SD-related EEG depression support this view, taken that SD plays a significant role in the pathophysiology of migraine (Brennan & Pietrobon, 2018). All things considered, the assessment of neurovascular coupling in migraine needs to be further explored and may possibly bear neurologic diagnostic value.

The impairment of functional hyperemia following SD has been suggested mechanistically linked to reduced CVR or the post-SD suppression of neural function (Piilgaard & Lauritzen, 2009). CVR is taken as a measure of endothelial dysfunction and the ability of cerebral vessels to dilate in response to a chemical stimulus causing nitric oxide release. The impairment of CVR assessed with hypercapnic challenge was found to persist for over an hour after SD in anesthetized rodents (Akin & Bilensoy, 2006; Fabricius et al., 1995; Florence et al., 1994; Lacombe et al., 1992), and breath holding during the inter-ictal period also attested diminishing CVR in migraineurs (Akin & Bilensoy, 2006; Dzator et al., 2021). Persistent vasoconstrictive tone underlying post-SD spreading oligemia, which is thought to be mediated by 20-hydroxy-eicosatetraenoic acid (20-HETE) or cyclooxygenase-1- (COX-1) and COX-2-derived prostanoids (Fordsmann et al., 2013; Gariepy et al., 2017) may also restrain post-SD vasodilation. In our study, the amplitude of functional hyperemia proved to be proportional to EVP amplitude after SD (Figure 4b), which suggests that the post-SD suppression of neural activity must have been implicated, at least in part, in the attenuation of the CBF response. Also, functional hyperemia amplitude was increasing together with the gradual recovery of CBF from post-SD oligemia (Figure 3d). This is thought to indicate that the progressive resolution of the sustained post-SD vasoconstriction probably allowed for the evolution of the functional hyperemic response. In conclusion, both post-SD suppression of neural activity and post-SD vasoconstrictive tone could possibly contribute to the weakening of functional hyperemia shortly after SD in our model.

4.2 | The impact of nimodipine

Prophylactic treatment with nimodipine appeared effective at reducing migraine headache frequency and severity in some earlier clinical trials (Battistella et al., 1990; Gelmers, 1983; Havanka-Kanniainen et al., 1985). Nimodipine has been best known for its anti-vasoconstrictor effect in cerebral vessels (Freedman & Waters, 1987), and was proposed to alleviate migraine by counteracting cerebral vasoconstriction (Leone et al., 1990). Furthermore, L-type VGCCs, the targets of nimodipine were implicated in calcitonin gene-related peptide (CGRP) release in the trigeminovascular system, a central element of the pain pathway in migraine (Amrutkar et al., 2011). Still, nimodipine's action on SD in the context of migraine remained elusive. In our experiments, pre-treatment with nimodipine

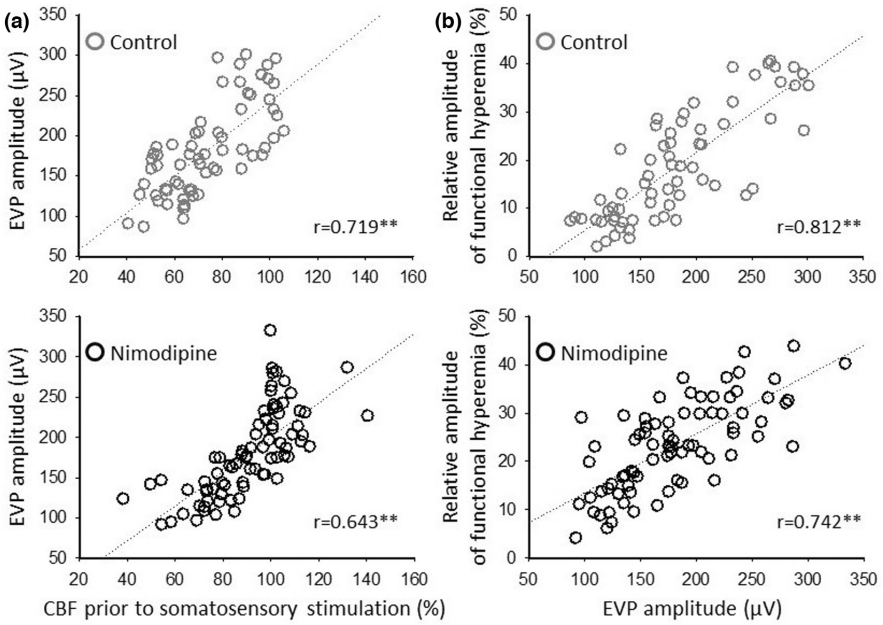

FIGURE 4 Correlation between resting pre-stimulus cerebral blood flow (CBF) and somatosensory evoked potential (EVP) amplitude (a), and EVP amplitude and the relative amplitude of the coupled functional hyperemia (b). A two-tailed Pearson correlation analysis was applied, $p < 0.01^{**}$.

exerted a tendency to shorten the SD-related EEG depression (Figure 2). Shorter SD duration achieved by nimodipine administration was previously reported in acute brain injury states, including experimental cerebral ischemia (Szabó et al., 2019; Tóth et al., 2020) and some patients of aneurysmal subarachnoid hemorrhage (SAH) (Carlson et al., 2021). Nimodipine may directly act on neuronal L-type VGCCs (Gould et al., 1985; Scriabine et al., 1989), but it is not likely that the facilitated restoration of spontaneous neural activity (EEG) was realized by direct nimodipine action, because nimodipine blocks slow inward calcium currents and suppresses neuronal (over)excitation (Scriabine & van den Kerckhoff, 1988). Also, nimodipine proved to be ineffective on the EVP amplitude during spreading oligemia here (Figure 3), consistent with our earlier finding in the ischemic cerebral cortex (Szabó et al., 2019). Taken together, the nimodipine-related accelerated recovery of the spontaneous neural activity from SD seen here must be secondary to CBF recovery from spreading oligemia. Indeed, the EEG power return was coincident with elevating CBF during spreading oligemia (Figure 2). Interestingly, the CBF minimum of spreading oligemia remained unaffected by nimodipine. The unchanged CBF minimum during spreading oligemia may be the reason why the beneficial effect of nimodipine on CBF recovery from post-SD spreading oligemia has been so far overlooked.

Nimodipine also attenuated the early hypoperfusion element of the CBF response to SD here (Figure 2). Of note, the early hypoperfusion component of the CBF response to SD is quite prominent in the mouse cortex as compared to the rat and other species, possibly because of a higher sensitivity of mouse cerebral vessels to vasoconstrictive potassium concentrations (Ayata et al., 2004; Ayata & Lauritzen, 2015). The attenuation of the hypoperfusion seen here is consistent with previous observations made in experimental rat models of subarachnoid hemorrhage that nimodipine antagonized the early and dominating vasoconstrictive element of the CBF response to arising SD (Dreier et al., 1998; Dreier et al., 2002). Furthermore, nimodipine reduced the SD-related early hypoperfusion potentiated with high extracellular K^+ concentration in the optimally perfused rat cortex (Menyhárt et al., 2018). The greater magnitude of the early vasoconstriction has been accepted to predict delayed repolarization after SD (Dreier, 2011). Following this argument, the attenuation of the early hypoperfusion element of the SD-coupled CBF response by nimodipine here could have contributed to the accelerated recovery of spontaneous neural activity from SD.

Finally, nimodipine augmented functional hyperemia indirectly, as the treatment increased the absolute—but not the relative—amplitude of the response because of the progressive resolution of spreading oligemia (Figure 3). This is consistent with earlier observations made in the optimally perfused rat cerebral cortex that nimodipine treatment increased baseline CBF from which functional hyperemia took off, thereby increasing the absolute amplitude of the flow response (Szabó et al., 2019). Nimodipine did not potentiate EVP or the relative amplitude of functional hyperemia when experimental groups were compared (Figure 3). According to the ANCOVA analysis, however, nimodipine appeared to interact with the efficacy of neurovascular coupling, the signaling mechanism adjusting the local CBF response to neural activity, by supporting greater hyperemia corresponding to smaller EVP amplitudes. Finally, the overall, absolute flow response to somatosensory stimulation peaked significantly higher after nimodipine treatment and was restored to baseline level sooner than in the control condition, which is considered beneficial, because the higher level of perfusion supports the more rapid return of neural function.

4.3 | Limitations

The choice of mice for this study may be perceived as a limitation. The late oligemic element of the CBF response to SD is usually more pronounced in mice than in phylogenetically higher mammals such as humans (Dreier & Reiffurth, 2015). Although vasoconstriction is

implicated to a greater extent in the hemodynamic response to SD in the naïve mouse brain, CBF is still sufficient to provide the energy required to initiate rapid repolarization of neurons and restoration of ion gradients to terminate SD. Therefore, SD in mice in naïve tissue does not last markedly longer than in higher mammals despite more pronounced vasoconstriction. The greater post-SD oligemia in the mouse and its reliable detection may, in fact, be considered as an opportunity to investigate the phenomenon in more detail.

5 | CONCLUSION

In conclusion, here we demonstrate that neurovascular coupling becomes reversibly impaired after SD, and gradually recovers over an hour after SD. We postulate that both the suppression of neural activity and the vasoconstrictive tone persistent after SD contribute to the impairment of functional hyperemia. We also show that nimodipine pre-treatment facilitates CBF recovery from spreading oligemia and attenuates the early hypoperfusion element of the CBF response to SD. Furthermore, nimodipine tends to shorten the SD-related EEG depression, which must originate in the nimodipine-linked elevation of CBF. Finally, nimodipine elevates the level of functional hyperemia and restores it more rapidly, which must be related to the acceleration of CBF recovery from spreading oligemia.

Migraine aura, which is thought to be linked to SD, is part of the clinical presentation of up to a third of migraine patients (Ferrari et al., 2022). Patients often report visual aura symptoms; in addition, sensory loss, dysphasia, and altered olfaction are also common (Hansen et al., 2016). The nimodipine-related facilitated recovery of neurovascular coupling and spontaneous neural activity after SD may offer the opportunity to reduce aura burden. In view of the presented experimental data, and taken the developments in pharmaceutical technology (Heng, 2018; Tóth et al., 2020) and personalized medicine, the use of nimodipine in migraine prophylaxis (especially with a focus on a rapid recovery from aura) is suggested to be re-visited.

AUTHOR CONTRIBUTIONS

ÁM designed the study; PK and ÁM conducted experiments and acquired data; PK, ARB, ÁM, and EF analyzed data; FB and EF supervised the work and provided funding; EF wrote the manuscript.

ACKNOWLEDGMENTS

This work was supported by the EU's Horizon 2020 research and innovation program under grant agreement No. 739593; grants from the National Research, Development and Innovation Office of Hungary (No. K134377 and K134334); the Ministry of Innovation and Technology of Hungary and the National Research, Development and Innovation Fund (No. TKP2021-EGA-28 financed under the TKP2021-EGA funding scheme); the Ministry of Human Capacities of Hungary (ÚNKP-20-4 -SZTE-153 and ÚNKP-22-2 –SZTE-225), and the University of Szeged Open Access Fund (nr. 5978). We are grateful to Dr. Ferenc Rárosi for advice in Biostatistics.

CONFLICT OF INTEREST STATEMENT

The authors declare that there are no known competing financial interests or personal relationships that relate to the research described in this paper.

DATA AVAILABILITY STATEMENT

Raw data are available from the First and Corresponding Authors on reasonable request.

ORCID

Ákos Menyhárt https://orcid.org/0000-0002-1355-3208
Eszter Farkas https://orcid.org/0000-0002-8478-9664

REFERENCES

Ahmadi, S., Ebrahimi, S. S., Oryan, S., & Rafieenia, F. (2012). Blockades of ATP-sensitive potassium channels and L-type calcium channels improve analgesic effect of morphine in alloxan-induced diabetic mice. *Pathophysiology*, *19*(3), 171–177. https://doi.org/10.1016/j.pathophys.2012.04.007

Akin, A., & Bilensoy, D. (2006). Cerebrovascular reactivity to hypercapnia in migraine patients measured with near-infrared spectroscopy. *Brain Research*, *1107*(1), 206–214. https://doi.org/10.1016/j.brainres.2006.06.002

Amrutkar, D. V., Ploug, K. B., Olesen, J., & Jansen-Olesen, I. (2011). Role for voltage gated calcium channels in calcitonin gene-related peptide release in the rat trigeminovascular system. *Neuroscience*, *172*, 510–517. https://doi.org/10.1016/j.neuroscience.2010.10.032

Ayata, C., & Lauritzen, M. (2015). Spreading depression, spreading depolarizations, and the cerebral vasculature. *Physiological Reviews*, *95*(3), 953–993. https://doi.org/10.1152/physrev.00027.2014

Ayata, C., Shin, H. K., Salomone, S., Ozdemir-Gursoy, Y., Boas, D. A., Dunn, A. K., & Moskowitz, M. A. (2004). Pronounced hypoperfusion during spreading depression in mouse cortex. *Journal of Cerebral Blood Flow and Metabolism*, *24*(10), 1172–1182. https://doi.org/10.1097/01.WCB.0000137057.92786.F3

Balkaya, M., Seidel, J. L., Sadeghian, H., Qin, T., Chung, D. Y., Eikermann-Haerter, K., van den Maagdenberg, A., Ferrari, M. D., & Ayata, C. (2019). Relief following chronic stress augments spreading depolarization susceptibility in familial hemiplegic migraine mice. *Neuroscience*, *415*, 1–9. https://doi.org/10.1016/j.neuroscience.2019.07.006

Battistella, P. A., Ruffilli, R., Moro, R., Fabiani, M., Bertoli, S., Antolini, A., & Zacchello, F. (1990). A placebo-controlled crossover trial of nimodipine in pediatric migraine. *Headache*, *30*(5), 264–268. https://doi.org/10.1111/j.1526-4610.1990.hed3005264.x

Böhm, M., Chung, D. Y., Gómez, C. A., Qin, T., Takizawa, T., Sadeghian, H., Sugimoto, K., Sakadžić, S., Yaseen, M. A., & Ayata, C. (2020). Neurovascular coupling during optogenetic functional activation: Local and remote stimulus-response characteristics, and uncoupling by spreading depression. *Journal of Cerebral Blood Flow and Metabolism*, *40*(4), 808–822. https://doi.org/10.1177/0271678X19845934

Brennan, K. C., & Pietrobon, D. (2018). A systems neuroscience approach to migraine. *Neuron*, *97*(5), 1004–1021. https://doi.org/10.1016/j.neuron.2018.01.029

Carlson, A. P., Alchbli, A., Hanggi, D., Macdonald, R. L., & Shuttleworth, C. W. (2021). Effect of locally delivered Nimodipine microparticles on spreading depolarization in aneurysmal subarachnoid hemorrhage. *Neurocritical Care*, *34*(1), 345–349. https://doi.org/10.1007/s12028-020-00935-1

Carlson, A. P., Hanggi, D., Macdonald, R. L., & Shuttleworth, C. W. (2020). Nimodipine reappraised: An old drug with a future. *Current Neuropharmacology*, *18*(1), 65–82. https://doi.org/10.2174/1570159X17666190927113021

Dreier, J. P. (2011). The role of spreading depression, spreading depolarization and spreading ischemia in neurological disease. *Nature Medicine*, *17*(4), 439–447. https://doi.org/10.1038/nm.2333

Dreier, J. P., Korner, K., Ebert, N., Gorner, A., Rubin, I., Back, T., Lindauer, U., Wolf, T., Villringer, A., Einhäupl, K. M., Lauritzen, M., & Dirnagl, U. (1998). Nitric oxide scavenging by hemoglobin or nitric oxide synthase inhibition by N-nitro-L-arginine induces cortical spreading ischemia when K+ is increased in the subarachnoid space. *Journal of Cerebral Blood Flow and Metabolism*, *18*(9), 978–990. https://doi.org/10.1097/00004647-199809000-00007

Dreier, J. P., & Reiffurth, C. (2015). The stroke-migraine depolarization continuum. *Neuron*, *86*(4), 902–922. https://doi.org/10.1016/j.neuron.2015.04.004

Dreier, J. P., Windmuller, O., Petzold, G., Lindauer, U., Einhaupl, K. M., & Dirnagl, U. (2002). Ischemia triggered by red blood cell products in the subarachnoid space is inhibited by nimodipine administration or moderate volume expansion/hemodilution in rats. *Neurosurgery*, *51*(6), 1457–1465 discussion 1465-1457.

Dreier, J. P., Winkler, M. K. L., Major, S., Horst, V., Lublinsky, S., Kola, V., Lemale, C. L., Kang, E. J., Maslarova, A., Salur, I., Lückl, J., Platz, J., Jorks, D., Oliveira-Ferreira, A. I., Schoknecht, K., Reiffurth, C., Milakara, D., Wiesenthal, D., Hecht, N., … Woitzik, J. (2022). Spreading depolarizations in ischaemia after subarachnoid haemorrhage, a diagnostic phase III study. *Brain*, *145*(4), 1264–1284. https://doi.org/10.1093/brain/awab457

Dzator, J. S., Howe, P. R., & Wong, R. H. (2021). Profiling cerebrovascular function in migraine: A systematic review and meta-analysis. *Journal of Cerebral Blood Flow and Metabolism*, *41*(5), 919–944. https://doi.org/10.1177/0271678X20964344

Enager, P., Gold, L., & Lauritzen, M. (2004). Impaired neurovascular coupling by transhemispheric diaschisis in rat cerebral cortex. *Journal of Cerebral Blood Flow and Metabolism*, *24*(7), 713–719. https://doi.org/10.1097/01.WCB.0000121233.63924.41

Fabricius, M., Akgoren, N., & Lauritzen, M. (1995). Arginine-nitric oxide pathway and cerebrovascular regulation in cortical spreading depression. *American Journal of Physiology*, *269*(1 Pt 2), H23–H29. https://doi.org/10.1152/ajpheart.1995.269.1.H23

Feigin, V. L., Rinkel, G. J., Algra, A., Vermeulen, M., & van Gijn, J. (1998). Calcium antagonists in patients with aneurysmal subarachnoid hemorrhage: A systematic review. *Neurology*, *50*(4), 876–883. https://doi.org/10.1212/wnl.50.4.876

Ferrari, M. D., Goadsby, P. J., Burstein, R., Kurth, T., Ayata, C., Charles, A., Ashina, M., van den Maagdenberg, A. M. J. M., & Dodick, D. W. (2022). Migraine. *Nature Reviews Disease Primers*, *8*(1), 2. https://doi.org/10.1038/s41572-021-00328-4

Florence, G., Bonvento, G., Charbonne, R., & Seylaz, J. (1994). Spreading depression reversibly impairs autoregulation of cortical blood flow. *American Journal of Physiology*, *266*(4 Pt 2), R1136–R1140. https://doi.org/10.1152/ajpregu.1994.266.4.R1136

Fordsmann, J. C., Ko, R. W., Choi, H. B., Thomsen, K., Witgen, B. M., Mathiesen, C., Lønstrup, M., Piilgaard, H., MacVicar, B., & Lauritzen, M. (2013). Increased 20-HETE synthesis explains reduced cerebral blood flow but not impaired neurovascular coupling after cortical spreading depression in rat cerebral cortex. *Journal of Neuroscience*, *33*(6), 2562–2570. https://doi.org/10.1523/JNEUROSCI.2308-12.2013

Fox, P. T., & Raichle, M. E. (1985). Stimulus rate determines regional brain blood flow in striate cortex. *Annals of Neurology*, *17*(3), 303–305. https://doi.org/10.1002/ana.410170315

Freedman, D. D., & Waters, D. D. (1987). 'Second generation' dihydropyridine calcium antagonists. Greater vascular selectivity and some unique applications. *Drugs*, *34*(5), 578–598. https://doi.org/10.2165/00003495-198734050-00005

Gariepy, H., Zhao, J., & Levy, D. (2017). Differential contribution of COX-1 and COX-2 derived prostanoids to cortical spreading depression-evoked cerebral oligemia. *Journal of Cerebral Blood Flow and Metabolism*, *37*(3), 1060–1068. https://doi.org/10.1177/0271678X16650217

Gelmers, H. J. (1983). Nimodipine, a new calcium antagonist, in the prophylactic treatment of migraine. *Headache*, *23*(3), 106–109. https://doi.org/10.1111/j.1526-4610.1983.hed2303106.x

Gould, R. J., Murphy, K. M., & Snyder, S. H. (1985). Autoradiographic localization of calcium channel antagonist receptors in rat brain with [3H]nitrendipine. *Brain Research*, *330*(2), 217–223. https://doi.org/10.1016/0006-8993(85)90680-8

Hadjikhani, N., Sanchez del Rio, M., Wu, O., Schwartz, D., Bakker, D., Fischl, B., Kwong, K. K., Cutrer, F. M., Rosen, B. R., Tootell, R. B., Sorensen, A. G., & Moskowitz, M. A. (2001). Mechanisms of migraine aura revealed by functional MRI in human visual cortex. *Proceedings of the National Academy of Sciences of the United States of America*, *98*(8), 4687–4692. https://doi.org/10.1073/pnas.071582498

Hansen, J. M., Goadsby, P. J., & Charles, A. C. (2016). Variability of clinical features in attacks of migraine with aura. *Cephalalgia*, *36*(3), 216–224. https://doi.org/10.1177/0333102415584601

Harriott, A. M., Chung, D. Y., Uner, A., Bozdayi, R. O., Morais, A., Takizawa, T., Qin, T., & Ayata, C. (2021). Optogenetic spreading depression elicits trigeminal pain and anxiety behavior. *Annals of Neurology*, *89*(1), 99–110. https://doi.org/10.1002/ana.25926

Havanka-Kanniainen, H., Hokkanen, E., & Myllyla, V. V. (1985). Efficacy of nimodipine in the prophylaxis of migraine. *Cephalalgia*, *5*(1), 39–43. https://doi.org/10.1046/j.1468-2982.1985.0501039.x

Heng, P. W. S. (2018). Controlled release drug delivery systems. *Pharmaceutical Development and Technology*, *23*(9), 833. https://doi.org/10.1080/10837450.2018.1534376

Herreras, O., Largo, C., Ibarz, J. M., Somjen, G. G., & Martin del Rio, R. (1994). Role of neuronal synchronizing mechanisms in the propagation of spreading depression in the in vivo hippocampus. *Journal of Neuroscience*, *14*(11 Pt 2), 7087–7098. https://doi.org/10.1523/JNEUROSCI.14-11-07087.1994

Howarth, C., Mishra, A., & Hall, C. N. (2021). More than just summed neuronal activity: How multiple cell types shape the BOLD response. *Philosophical Transactions of the Royal Society of London. Series B: Biological Sciences*, *376*(1815), 20190630. https://doi.org/10.1098/rstb.2019.0630

Ingwersen, J., De Santi, L., Wingerath, B., Graf, J., Koop, B., Schneider, R., Hecker, C., Schröter, F., Bayer, M., Engelke, A. D., Dietrich, M., Albrecht, P., Hartung, H. P., Annunziata, P., Aktas, O., & Prozorovski, T. (2018). Nimodipine confers clinical improvement in two models of experimental autoimmune encephalomyelitis. *Journal of Neurochemistry*, *146*, 86–98. https://doi.org/10.1111/jnc.14324

Lacombe, P., Sercombe, R., Correze, J. L., Springhetti, V., & Seylaz, J. (1992). Spreading depression induces prolonged reduction of cortical blood flow reactivity in the rat. *Experimental Neurology*, *117*(3), 278–286. https://doi.org/10.1016/0014-4886(92)90137-f

Langdon, R. B., & Sur, M. (1990). Components of field potentials evoked by white matter stimulation in isolated slices of primary visual cortex: Spatial distributions and synaptic order. *Journal of Neurophysiology*, *64*(5), 1484–1501. https://doi.org/10.1152/jn.1990.64.5.1484

Lashley, K. S. (1941). Patterns of cerebral integration indicated by the scotomas of migraine. *Archives of Neurology and Psychiatry*, *46*, 331–339.

Lauritzen, M. (1994). Pathophysiology of the migraine aura. The spreading depression theory. *Brain*, *117*(Pt 1), 199–210. https://doi.org/10.1093/brain/117.1.199

Lauritzen, M., Skyhoj Olsen, T., Lassen, N. A., & Paulson, O. B. (1983). Changes in regional cerebral blood flow during the course of classic migraine attacks. *Annals of Neurology*, *13*(6), 633–641. https://doi.org/10.1002/ana.410130609

Leao, A. A. P. (1944). Spreading depression of activity in the cerebral cortex. *Journal of Neurophysiology*, *7*, 359–390.

Leao, A. A. P., & Morison, R. S. (1945). Propagation of spreading cortical depression. *Journal of Neurophysiology*, *8*, 33–45. https://doi.org/10.1152/jn.1945.8.1.33

Leone, M., Frediani, F., Patruno, G., Valentini, S., & Bussone, G. (1990). Is nimodipine useful in migraine prophylaxis? Further considerations. *Headache*, *30*(6), 363–365. https://doi.org/10.1111/j.1526-4610.1990.hed3006363.x

Lo, Y. L., Wee, S. L., Zhao, Y. J., & Narasimhalu, K. (2020). Interictal hemodynamic abnormality during motor activation in sporadic hemiplegic migraine: An explorative study. *Journal of the Neurological Sciences*, *418*, 117148. https://doi.org/10.1016/j.jns.2020.117148

Lückl, J., Lemale, C. L., Kola, V., Horst, V., Khojasteh, U., Oliveira-Ferreira, A. I., Major, S., Winkler, M. K. L., Kang, E. J., Schoknecht, K., Martus, P., Hartings, J. A., Woitzik, J., & Dreier, J. P. (2018). The negative ultraslow potential, electrophysiological correlate of infarction in the human cortex. *Brain*, *141*(6), 1734–1752. https://doi.org/10.1093/brain/awy102

Menyhárt, Á., Farkas, A. E., Varga, D. P., Frank, R., Tóth, R., Bálint, A. R., Makra, P., Dreier, J. P., Bari, F., Krizbai, I. A., & Farkas, E. (2018). Large-conductance Ca^{2+}-activated potassium channels are potently involved in the inverse neurovascular response to spreading depolarization. *Neurobiology of Disease*, *119*, 41–52. https://doi.org/10.1016/j.nbd.2018.07.026

Menyhárt, Á., Frank, R., Farkas, A. E., Süle, Z., Varga, V. É., Nyúl-Tóth, Á., Meiller, A., Ivánkovits-Kiss, O., Lemale, C. L., Szabó, Í., Tóth, R., Zölei-Szénási, D., Woitzik, J., Marinesco, S., Krizbai, I. A., Bari, F., Dreier, J. P., & Farkas, E. (2021). Malignant astrocyte swelling and impaired glutamate clearance drive the expansion of injurious spreading depolarization foci. *Journal of Cerebral Blood Flow and Metabolism*, *42*, 584–599. https://doi.org/10.1177/0271678X211040056

Migraine-Nimodipine European Study Group (MINES). (1989a). European multicenter trial of nimodipine in the prophylaxis of classic migraine (migraine with aura). *Headache*, *29*(10), 639–642.

Migraine-Nimodipine European Study Group (MINES). (1989b). European multicenter trial of nimodipine in the prophylaxis of common migraine (migraine without aura). *Headache*, *29*(10), 633–638.

Milner, P. M. (1958). Note on a possible correspondence between the scotomas of migraine and spreading depression of Leao. *Electroencephalography and Clinical Neurophysiology*, *10*(4), 705. https://doi.org/10.1016/0013-4694(58)90073-7

Olesen, J., Larsen, B., & Lauritzen, M. (1981). Focal hyperemia followed by spreading oligemia and impaired activation of rCBF in classic migraine. *Annals of Neurology*, *9*(4), 344–352. https://doi.org/10.1002/ana.410090406

Percie du Sert, N., Hurst, V., Ahluwalia, A., Alam, S., Avey, M. T., Baker, M., Browne, W. J., Clark, A., Cuthill, I. C., Dirnagl, U., Emerson, M., Garner, P., Holgate, S. T., Howells, D. W., Karp, N. A., Lazic, S. E., Lidster, K., MacCallum, C., Macleod, M., … Würbel, H. (2020). The ARRIVE guidelines 2.0: Updated guidelines for reporting animal research. *Journal of Cerebral Blood Flow and Metabolism*, *40*(9), 1769–1777. https://doi.org/10.1177/0271678X20943823

Piilgaard, H., & Lauritzen, M. (2009). Persistent increase in oxygen consumption and impaired neurovascular coupling after spreading depression in rat neocortex. *Journal of Cerebral Blood Flow and Metabolism*, *29*(9), 1517–1527. https://doi.org/10.1038/jcbfm.2009.73

Scriabine, A., Schuurman, T., & Traber, J. (1989). Pharmacological basis for the use of nimodipine in central nervous system disorders. *FASEB Journal*, *3*(7), 1799–1806.

Scriabine, A., & van den Kerckhoff, W. (1988). Pharmacology of nimodipine. A review. *Annals of the new York Academy of Sciences*, *522*, 698–706. https://doi.org/10.1111/j.1749-6632.1988.tb33415.x

Somjen, G. G. (2001). Mechanisms of spreading depression and hypoxic spreading depression-like depolarization. *Physiological Reviews*, *81*(3), 1065–1096. https://doi.org/10.1152/physrev.2001.81.3.1065

Stackhouse, T. L., & Mishra, A. (2021). Neurovascular coupling in development and disease: Focus on astrocytes. *Frontiers in Cell and Development Biology*, *9*, 702832. https://doi.org/10.3389/fcell.2021.702832

Szabó, Í., Tóth, O. M., Török, Z., Varga, D. P., Menyhárt, Á., Frank, R., Hantosi, D., Hunya, Á., Bari, F., Horváth, I., Vigh, L., & Farkas, E. (2019). The impact of dihydropyridine derivatives on the cerebral blood flow response to somatosensory stimulation and spreading depolarization. *British Journal of Pharmacology*, *176*(9), 1222–1234. https://doi.org/10.1111/bph.14611

Szabó, Í., Varga, V. E., Dvorácskó, S., Farkas, A. E., Körmöczi, T., Berkecz, R., Kecskés, S., Menyhárt, Á., Frank, R., Hantosi, D., Cozzi, N. V., Frecska, E., Tömböly, C., Krizbai, I. A., Bari, F., & Farkas, E. (2021). N,N-dimethyltryptamine attenuates spreading depolarization and restrains neurodegeneration by sigma-1 receptor activation in the ischemic rat brain. *Neuropharmacology*, *192*, 108612. https://doi.org/10.1016/j.neuropharm.2021.108612

Toldo, I., De Carlo, D., Bolzonella, B., Sartori, S., & Battistella, P. A. (2012). The pharmacological treatment of migraine in children and adolescents: An overview. *Expert Review of Neurotherapeutics*, *12*(9), 1133–1142. https://doi.org/10.1586/ern.12.104

Tóth, O. M., Menyhárt, Á., Varga, V. E., Hantosi, D., Ivánkovits-Kiss, O., Varga, D. P., Szabó, Í., Janovák, L., Dékány, I., Farkas, E., & Bari, F. (2020). Chitosan nanoparticles release nimodipine in response to tissue acidosis to attenuate spreading depolarization evoked during forebrain ischemia. *Neuropharmacology*, *162*, 107850. https://doi.org/10.1016/j.neuropharm.2019.107850

Toth, R., Farkas, A. E., Krizbai, I. A., Makra, P., Bari, F., Farkas, E., & Menyhart, A. (2021). Astrocyte Ca^{2+} waves and subsequent non-synchronized Ca^{2+} oscillations coincide with arteriole diameter changes in response to spreading depolarization. *International Journal of Molecular Sciences*, *22*(7). https://doi.org/10.3390/ijms22073442

Unekawa, M., Ikeda, K., Tomita, Y., Kawakami, K., & Suzuki, N. (2018). Enhanced susceptibility to cortical spreading depression in two types of Na^+, K^+-ATPase α2 subunit-deficient mice as a model of familial hemiplegic migraine 2. *Cephalalgia*, *38*(9), 1515–1524. https://doi.org/10.1177/0333102417738249

van den Maagdenberg, A. M., Pietrobon, D., Pizzorusso, T., Kaja, S., Broos, L. A., Cesetti, T., van de Ven, R., Tottene, A., van der Kaa, J., Plomp, J. J., Frants, R. R., & Ferrari, M. D. (2004). A Cacna1a knockin migraine mouse model with increased susceptibility to cortical spreading depression. *Neuron*, *41*(5), 701–710. https://doi.org/10.1016/s0896-6273(04)00085-6

Wahl, M., Lauritzen, M., & Schilling, L. (1987). Change of cerebrovascular reactivity after cortical spreading depression in cats and rats. *Brain Research*, *411*(1), 72–80. https://doi.org/10.1016/0006-8993(87)90682-2

Windmuller, O., Lindauer, U., Foddis, M., Einhaupl, K. M., Dirnagl, U., Heinemann, U., & Dreier, J. P. (2005). Ion changes in spreading ischaemia induce rat middle cerebral artery constriction in the absence of NO. *Brain*, *128*(Pt 9), 2042–2051. https://doi.org/10.1093/brain/awh545

Woods, R. P., Iacoboni, M., & Mazziotta, J. C. (1994). Brief report: Bilateral spreading cerebral hypoperfusion during spontaneous migraine headache. *New England Journal of Medicine*, *331*(25), 1689–1692. https://doi.org/10.1056/NEJM199412223312505

How to cite this article: Menyhárt, Á., Bálint, A. R., Kozák, P., Bari, F., & Farkas, E. (2024). Nimodipine accelerates the restoration of functional hyperemia during spreading oligemia. *Journal of Neurochemistry*, *168*, 888–898. https://doi.org/10.1111/jnc.15792